

Type III migration in a low viscosity disc

Min-Kai Lin

Supervisor: John Papaloizou

DAMTP

University of Cambridge

AMNH, New York, January 19, 2010

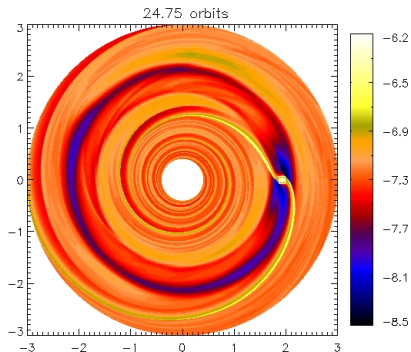


Outline

- ▶ Introduction: planet migration types
- ▶ Numerical methods, first results and motivation
- ▶ Type III migration in an inviscid disc:
 - ▶ Formation of vortensity rings
 - ▶ Linear stability
 - ▶ Non-linear outcome and role in type III
- ▶ Conclusions
- ▶ Future work

Introduction

- ▶ 374 exo-planets discovered (2 October 2009).
- ▶ First 'hot Jupiter' around 51 Pegasi, orbital period 4 days (Mayor & Queloz 1995). Fomalhaut b with semi-major axis 115AU.
- ▶ Formation difficult in situ, so invoke *migration*: interaction of planet with gaseous disc (Goldreich & Tremaine 1979; Lin & Papaloizou 1986).





Type I and type II

- ▶ Type I: linear theory for small planet masses (Earths). Waves from Lindblad resonances ($\Omega(r_L) = \Omega_p \pm \kappa/m$) imply a torque on the disc

$$\Gamma_{\text{LR},m} = \frac{\text{sgn}(\Omega_p - \Omega)\pi^2\Sigma}{3\Omega\Omega_p} \times \left[r \frac{d\psi_m}{dr} + \frac{2m^2(\Omega - \Omega_p)}{\Omega} \psi_m \right]^2.$$

The linear co-rotation torque due to co-rotation resonance ($\Omega(r_C) = \Omega_p$)

$$\Gamma_{\text{CR},m} = \frac{\pi^2 m \psi_m^2}{2} \left(\frac{d\Omega}{dr} \right)^{-1} \frac{d}{dr} \left(\frac{\Sigma}{B} \right),$$

where $B = \omega/2$. No Γ_{CR} in Keplerian disc with $\Sigma \propto r^{-3/2}$.

- ▶ Type II: gap-opening for massive planets (Jovian). Migration locked with disc viscous evolution. Criteria: $r_p(M_p/3M_*)^{1/3} > H$ or $M_p/M_* > 40\nu/a^2\Omega$.



Type I and type II

- Type I: linear theory for small planet masses (Earths). Waves from Lindblad resonances ($\Omega(r_L) = \Omega_p \pm \kappa/m$) imply a torque on the disc

$$\Gamma_{\text{LR},m} = \frac{\text{sgn}(\Omega_p - \Omega)\pi^2\Sigma}{3\Omega\Omega_p} \times \left[r \frac{d\psi_m}{dr} + \frac{2m^2(\Omega - \Omega_p)}{\Omega} \psi_m \right]^2.$$

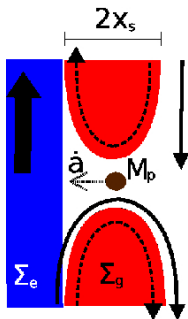
The linear co-rotation torque due to co-rotation resonance ($\Omega(r_C) = \Omega_p$)

$$\Gamma_{\text{CR},m} = \frac{\pi^2 m \psi_m^2}{2} \left(\frac{d\Omega}{dr} \right)^{-1} \frac{d}{dr} \left(\frac{\Sigma}{B} \right),$$

where $B = \omega/2$. No Γ_{CR} in Keplerian disc with $\Sigma \propto r^{-3/2}$.

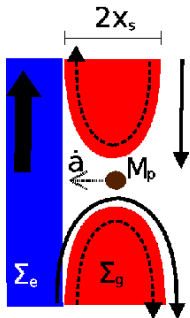
- Type II: gap-opening for massive planets (Jovian). Migration locked with disc viscous evolution. Criteria: $r_p(M_p/3M_*)^{1/3} > H$ or $M_p/M_* > 40\nu/a^2\Omega$.
- What about intermediate, Saturn-mass planets with partial gaps? There is another source of torque that depends on migration rate.

Physics of type III migration



- ▶ Fluid element orbital radius changes from $a - x_s \rightarrow a + x_s \Rightarrow$ torque on planet:

$$\Gamma_3 = 2\pi a^2 \dot{\Sigma}_e \Omega x_s.$$



- ▶ Fluid element orbital radius changes from $a - x_s \rightarrow a + x_s \Rightarrow$ torque on planet:

$$\Gamma_3 = 2\pi a^2 \dot{a} \Sigma_e \Omega x_s.$$

- ▶ Migration rate for $M_p + M_r + M_h$:

$$\dot{a} = \frac{2\Gamma_L}{\Omega a \underbrace{(M_p + M_r - \delta m)}_{M'_p}} \quad (1)$$

where Γ_L is the total Lindblad torque and

$$\delta m = 4\pi \Sigma_e a x_s - M_h = 4\pi a x_s (\Sigma_e - \Sigma_g)$$

is the density-defined co-orbital mass deficit.

- ▶ Co-orbital mass deficit:

larger $\delta m \Rightarrow$ faster migration.

- ▶ Horse-shoe width: x_s , separating co-orbital and circulating region. Take $x_s = 2.5r_h$ for result analysis ($r_h \equiv (M_p/3M_*)^{1/3}a$). Can show $x_s \lesssim 2.3r_h$ in particle dynamics limit.

- ▶ Vortensity: $\eta \equiv \omega/\Sigma$, important for stability properties and η^{-1} also used to define δm (Masset & Papaloizou 2003).

- ▶ Modelling assumptions: steady, slow migration ($\tau_{\text{lib}}/\tau_{\text{mig}} \ll 1$), horse-shoe material moves with planet.

Standard numerical setup for disc-planet interaction. 2D disc in polar co-ordinates centered on primary but non-rotating. Units $G = M_* = 1$.

- ▶ Hydrodynamic equations with local isothermal equation of state:

$$\frac{\partial \Sigma}{\partial t} + \nabla \cdot (\Sigma \mathbf{v}) = 0,$$

$$\frac{\partial v_r}{\partial t} + \mathbf{v} \cdot \nabla v_r - \frac{v_\phi^2}{r} = -\frac{1}{\Sigma} \frac{\partial P}{\partial r} - \frac{\partial \Phi}{\partial r} + \frac{f_r}{\Sigma},$$

$$\frac{\partial v_\phi}{\partial t} + \mathbf{v} \cdot \nabla v_\phi + \frac{v_\phi v_r}{r} = -\frac{1}{\Sigma r} \frac{\partial P}{\partial \phi} - \frac{1}{r} \frac{\partial \Phi}{\partial \phi} + \frac{f_\phi}{\Sigma},$$

$$P = c_s^2(r) \Sigma.$$

Viscous forces $f \propto \nu = \nu_0 \times 10^{-5}$, temperature $c_s^2 = h^2/r$, $h = H/r$. Φ is total potential including primary, planet (softening $\epsilon = 0.6H$), indirect terms but **no self-gravity**.

- ▶ Method: FARGO code (Masset 2000), finite difference for hydrodynamics, RK5 for planet motion.



Type III in action

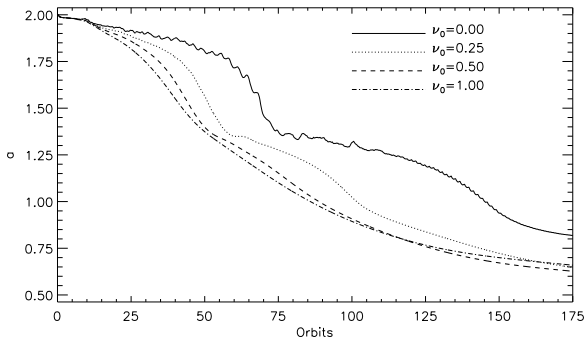
Discs: uniform density $\Sigma = 7 \times 10^{-4}$, aspect ratio $h = 0.05$ and different uniform kinematic viscosities.

Planet: Saturn mass $M_p = 2.8 \times 10^{-4}$ initially at $r = 2$.

Type III in action

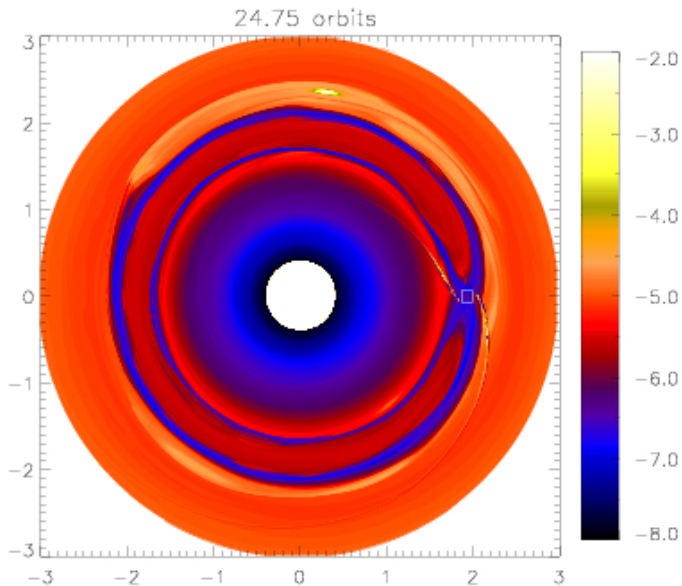
Discs: uniform density $\Sigma = 7 \times 10^{-4}$, aspect ratio $h = 0.05$ and different uniform kinematic viscosities.

Planet: Saturn mass $M_p = 2.8 \times 10^{-4}$ initially at $r = 2$.

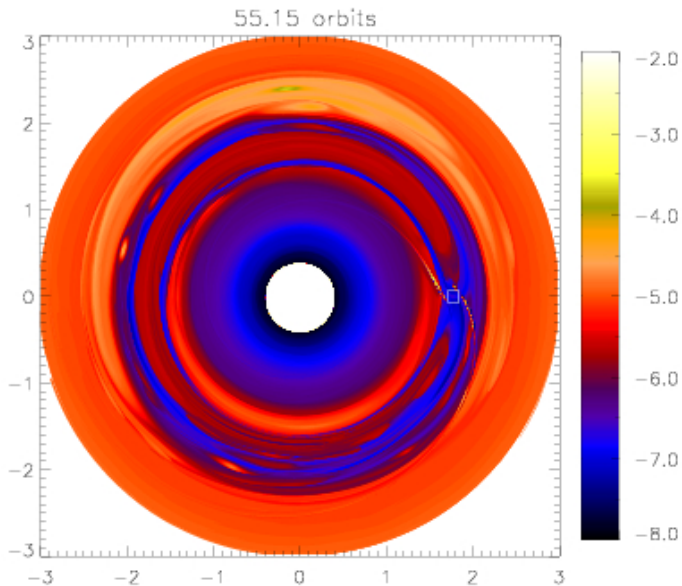


What's going on at low viscosities?

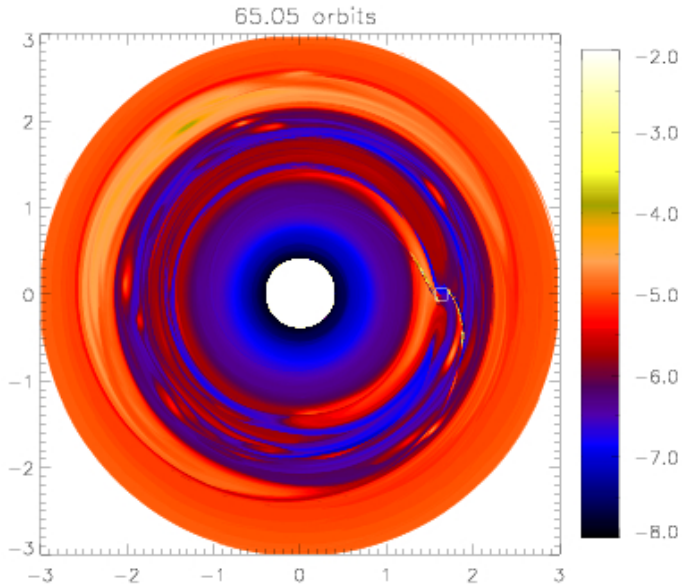
Inviscid case: evolution of Σ/ω :



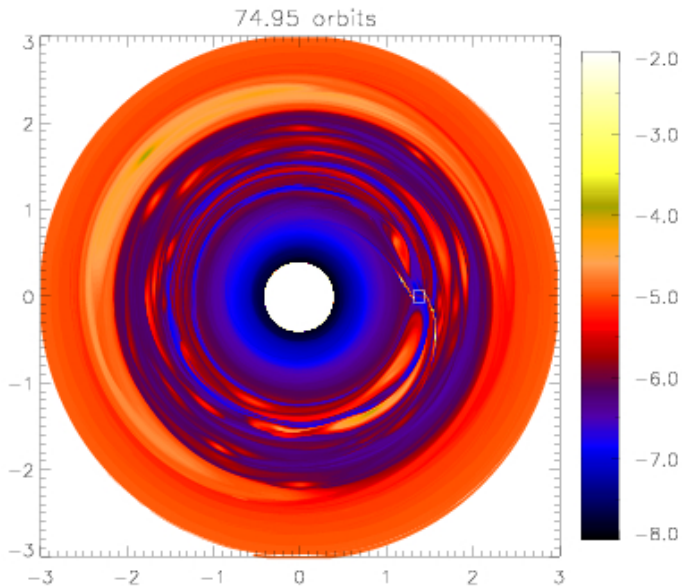
Inviscid case: evolution of Σ/ω :



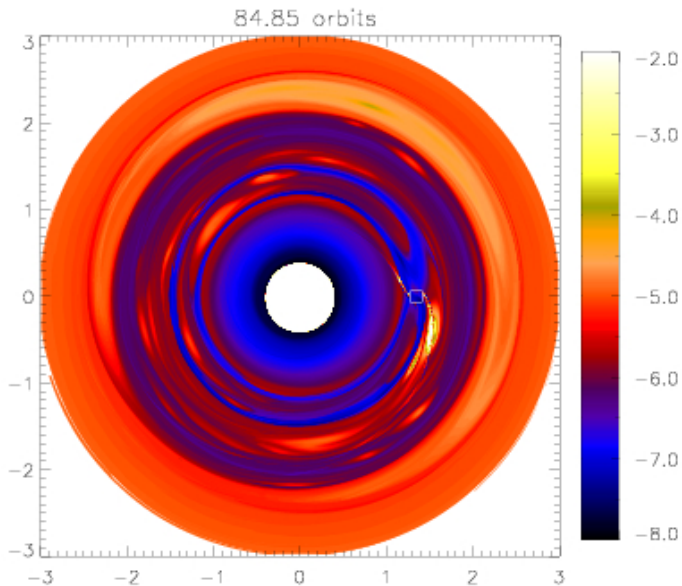
Inviscid case: evolution of Σ/ω :



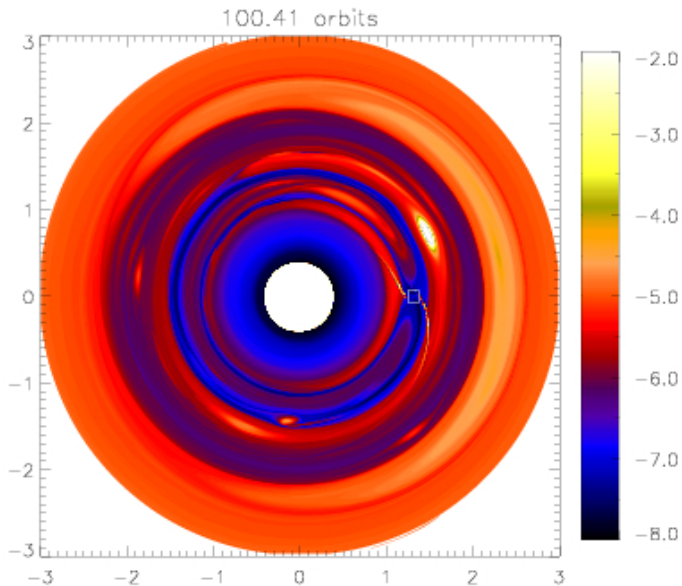
Inviscid case: evolution of Σ/ω :



Inviscid case: evolution of Σ/ω :

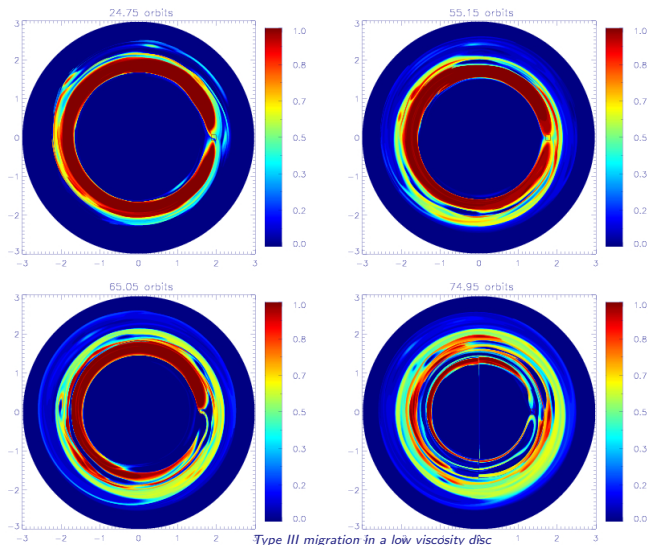


Inviscid case: evolution of Σ/ω :



Loss of horse-shoe material

Advection of passive scalar initially in $r = r_p \pm 2r_h$. $t_{\text{lib}}/t_{\text{mig}} \simeq 0.6$.



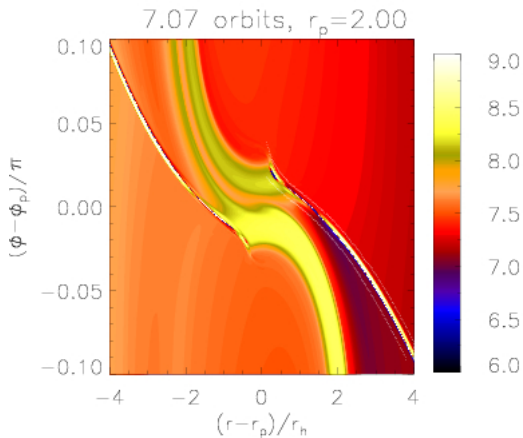
- ▶ Vortensity equation:

$$\left(\frac{\partial}{\partial t} + \mathbf{v} \cdot \nabla \right) \left(\frac{\omega}{\Sigma} \right) = \frac{dc_s^2}{dr} \frac{\partial}{\partial \phi} \left(\frac{1}{\Sigma} \right).$$

Axisymmetry and/or barotropic \Rightarrow vortensity conserved *except at shocks*.

- ▶ Confirmed by fixed-orbit, high resolution simulation ($r = [1, 3]$, $N_\phi \times N_r = 3072 \times 1024$) $\Delta r \simeq 0.02r_h$, $r\Delta\phi \simeq 0.05r_h$.

Vortensity rings: formation via shocks



Vortensity generated as fluid elements U-turn during its horse-shoe orbit.



Predicting the vortensity jump

We need:



Predicting the vortensity jump

We need:

- ▶ **Vortensity jump** across isothermal shock:

$$\left[\frac{\omega}{\Sigma} \right] = - \frac{(M^2 - 1)^2}{\Sigma M^4} \frac{\partial v_{\perp}}{\partial S} - \left(\frac{M^2 - 1}{\Sigma M^2 v_{\perp}} \right) \frac{\partial c_s^2}{\partial S}.$$

RHS is pre-shock. $M = v_{\perp}/c_s$, S is distance along shock (increasing radius). Additional baroclinic term compared to Li et al. (2005) but has negligible effect ($c_s^2 \propto 1/r$).



Predicting the vortensity jump

We need:

- ▶ **Vortensity jump** across isothermal shock:

$$\left[\frac{\omega}{\Sigma} \right] = - \frac{(M^2 - 1)^2}{\Sigma M^4} \frac{\partial v_{\perp}}{\partial S} - \left(\frac{M^2 - 1}{\Sigma M^2 v_{\perp}} \right) \frac{\partial c_s^2}{\partial S}.$$

RHS is pre-shock. $M = v_{\perp}/c_s$, S is distance along shock (increasing radius). Additional baroclinic term compared to Li et al. (2005) but has negligible effect ($c_s^2 \propto 1/r$).

- ▶ **Flow field**: shearing-box geometry, velocity field from zero-pressure momentum equations, density field from vortensity conservation following a particle.

Predicting the vortensity jump

We need:

- ▶ **Vortensity jump** across isothermal shock:

$$\left[\frac{\omega}{\Sigma} \right] = - \frac{(M^2 - 1)^2}{\Sigma M^4} \frac{\partial v_{\perp}}{\partial S} - \left(\frac{M^2 - 1}{\Sigma M^2 v_{\perp}} \right) \frac{\partial c_s^2}{\partial S}.$$

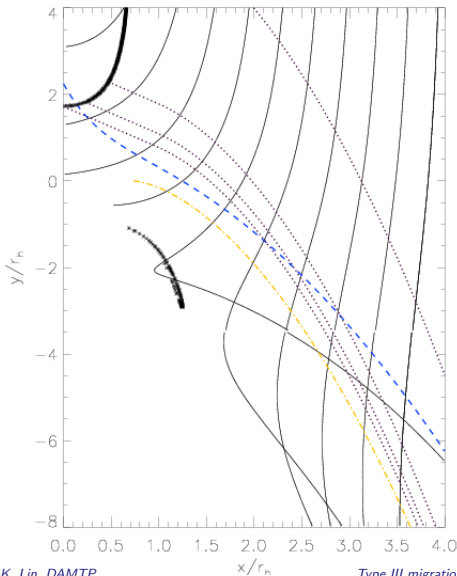
RHS is pre-shock. $M = v_{\perp}/c_s$, S is distance along shock (increasing radius). Additional baroclinic term compared to Li et al. (2005) but has negligible effect ($c_s^2 \propto 1/r$).

- ▶ **Flow field**: shearing-box geometry, velocity field from zero-pressure momentum equations, density field from vortensity conservation following a particle.
- ▶ **Shock location** : generalised Papaloizou et al. (2004)

$$\frac{dy_s}{dx} = \frac{\hat{v}_y^2 - 1}{\hat{v}_x \hat{v}_y - \sqrt{\hat{v}_x^2 + \hat{v}_y^2 - 1}}.$$

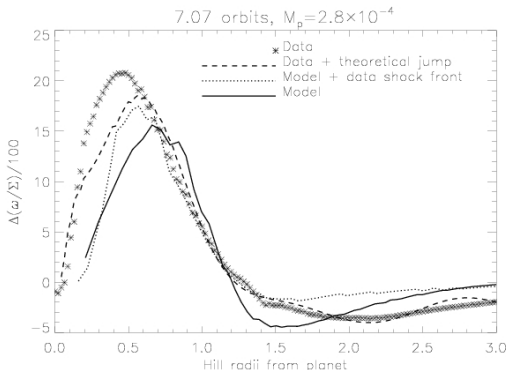
$$\hat{v} \equiv v/c_s.$$

Shock location



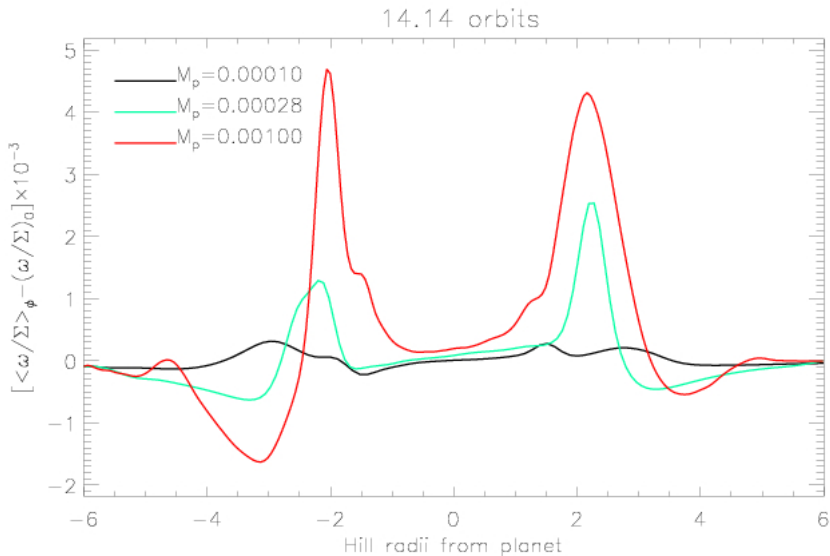
- ▶ Solid lines: particle paths from the zero-pressure momentum equations,
- ▶ Thick lines: sonic points $|\mathbf{v}| = c_s$,
- ▶ Dotted lines: theoretical shock fronts;
- ▶ Dash-dot: solution for Keplerian flow;
- ▶ Dashed : polynomial fit to simulation shock front.

The actual shock front begins around $x = 0.2r_h$, where it crosses the sonic point.



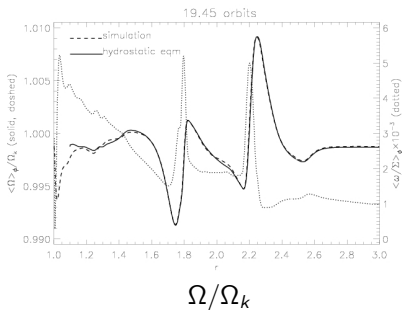
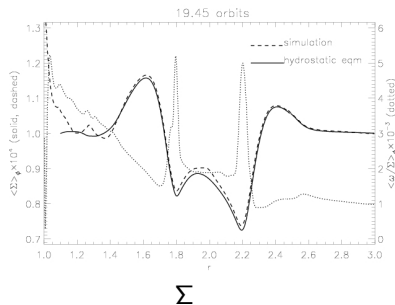
- ▶ Vortensity generation near shock tip (horse-shoe orbits) , vortensity destruction further away (circulating region). Variation in flow properties on scales of $r_h \simeq H$.
- ▶ Variation in disc profiles on scale-heights enables shear instability \Rightarrow vortices in non-linear stage (Lovelace et al. 1999, Li et al. 2001).

Vortensity generation v.s. M_p

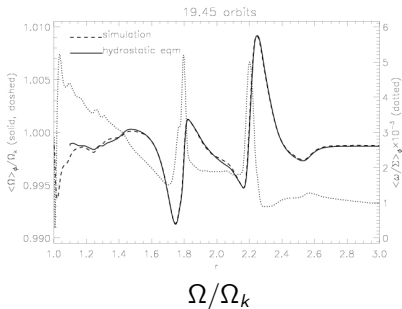
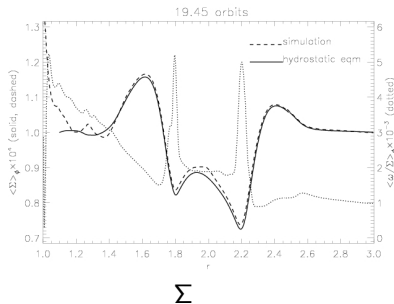


Ring stability

Idea: linear stability analysis of inviscid disc but use simulation vortensity profile as basic state: axisymmetric, $v_r = 0$.



Idea: linear stability analysis of inviscid disc but use simulation vortensity profile as basic state: axisymmetric, $v_r = 0$.



- ▶ In principle can predict gap structure via shock modelling / vortensity generation. Important to check axisymmetric hydrostatic basic state, otherwise linear analysis becomes very difficult.

- ▶ Governing equation for isothermal perturbations $\propto \exp i(\sigma t + m\phi)$:

$$\frac{d}{dr} \left(\frac{\Sigma}{\kappa^2 - \bar{\sigma}^2} \frac{dW}{dr} \right) + \left\{ \frac{m}{\bar{\sigma}} \frac{d}{dr} \left[\frac{\kappa^2}{r\eta(\kappa^2 - \bar{\sigma}^2)} \right] - \frac{r\Sigma}{h^2} - \frac{m^2\Sigma}{r^2(\kappa^2 - \bar{\sigma}^2)} \right\} W = 0$$

$$W = \delta\Sigma/\Sigma; \kappa^2 = 2\Sigma\eta\Omega; \bar{\sigma} = \sigma + m\Omega(r).$$

- ▶ Self-excited modes in inviscid disc with sharp vortensity profiles.

- ▶ Governing equation for isothermal perturbations $\propto \exp i(\sigma t + m\phi)$:

$$\frac{d}{dr} \left(\frac{\Sigma}{\kappa^2 - \bar{\sigma}^2} \frac{dW}{dr} \right) + \left\{ \frac{m}{\bar{\sigma}} \frac{d}{dr} \left[\frac{\kappa^2}{r\eta(\kappa^2 - \bar{\sigma}^2)} \right] - \frac{r\Sigma}{h^2} - \frac{m^2\Sigma}{r^2(\kappa^2 - \bar{\sigma}^2)} \right\} W = 0$$

$$W = \delta\Sigma/\Sigma; \quad \kappa^2 = 2\Sigma\eta\Omega; \quad \bar{\sigma} = \sigma + m\Omega(r).$$

- ▶ Self-excited modes in inviscid disc with sharp vortensity profiles.
- ▶ Simplified equation for "co-rotational modes" ($\kappa^2 \gg |\bar{\sigma}^2|$, $m = O(1)$):

$$\frac{d}{dr} \left(\frac{rc^2\Sigma}{\kappa^2} \frac{dW}{dr} \right) + \left\{ \frac{m}{\bar{\sigma}} \frac{d}{dr} \left[\frac{c^2}{\eta} \right] - r\Sigma \right\} W = 0.$$

Should have $(c^2/\eta)' \rightarrow 0$ as $\bar{\sigma} \rightarrow 0$ to stay regular.

- ▶ Multiply simplified equation by W^* , integrate then take imaginary part:

$$-i\gamma \int_{r_1}^{r_2} \frac{m}{(\sigma_R + m\Omega)^2 + \gamma^2} \left(\frac{c^2}{\eta}\right)' |W|^2 dr = 0$$

$\sigma = \sigma_R + i\gamma$. Must have $(c^2/\eta)' = 0$ at co-rotation point r_0 for non-neutral modes to exist ($\gamma \neq 0$). Shock-modified protoplanetary disc satisfies necessary condition.



Properties of co-rotational modes

- ▶ Multiply simplified equation by W^* , integrate then take imaginary part:

$$-i\gamma \int_{r_1}^{r_2} \frac{m}{(\sigma_R + m\Omega)^2 + \gamma^2} \left(\frac{c^2}{\eta}\right)' |W|^2 dr = 0$$

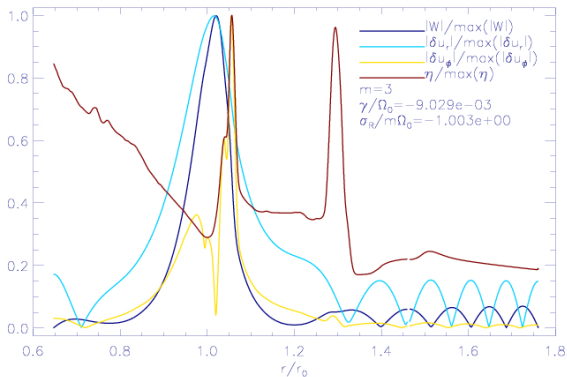
$\sigma = \sigma_R + i\gamma$. Must have $(c^2/\eta)' = 0$ at co-rotation point r_0 for non-neutral modes to exist ($\gamma \neq 0$). Shock-modified protoplanetary disc satisfies necessary condition.

- ▶ Semi-circle theorem. Define $W = g\bar{\sigma}$ then multiply by g^* and integrate. Can show (approximately):

$$\gamma^2 + \left[\sigma_R + \frac{1}{2}m(\Omega_+ + \Omega_-) \right]^2 \leq m^2 \left(\frac{\Omega_+ - \Omega_-}{2} \right)^2.$$

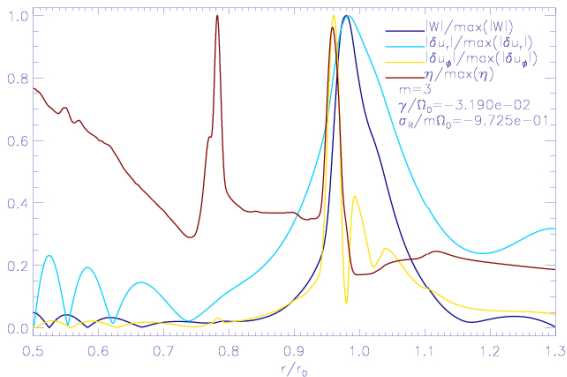
Ω_{\pm} are maximum and minimum angular speed in region of interest.
Growth rate limited by local shear.

Example: $m = 3$, $h = 0.05$



- ▶ Disturbance focused around vortensity minimum (gap edge), exponential decays either side joined by vortensity term at co-rotation r_0 . More extreme minimum \Rightarrow more localised.
- ▶ Waves beyond the Lindblad resonances ($\kappa^2 - \bar{\sigma}^2 = 0$) but amplitude not large compared to co-rotation.

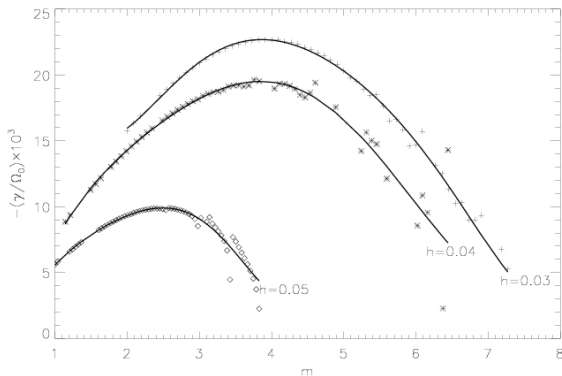
Example: $m = 3$, $h = 0.05$



- ▶ Disturbance focused around vortensity minimum (gap edge), exponential decays either side joined by vortensity term at co-rotation r_0 . More extreme minimum \Rightarrow more localised.
- ▶ Waves beyond the Lindblad resonances ($\kappa^2 - \bar{\sigma}^2 = 0$) but amplitude not large compared to co-rotation.

Growth rate v.s. m and h

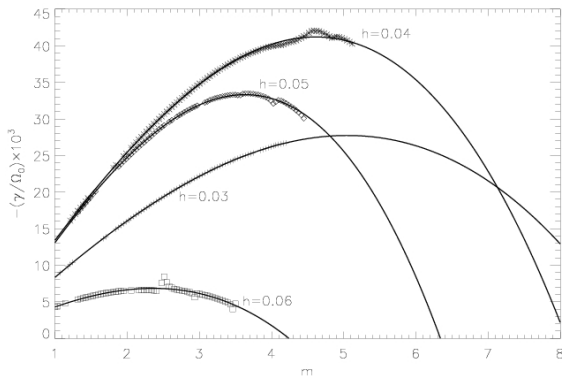
Solve for non-integer m to get dependence on γ on azimuthal wave-number. Polynomial fit.



Inner edge

$h = 0.05$, $T_{\text{grow}} \sim 10$ orbital periods at $r = 2$.

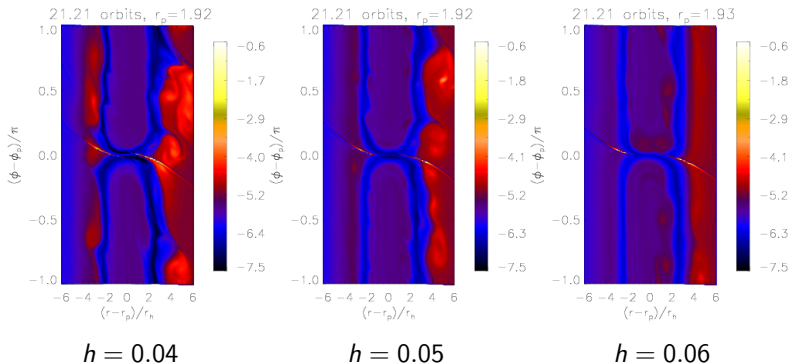
Growth rate v.s. m and h



Outer edge

($h = 0.03$ spurious, $\eta(r)$ not representative of disc.)

Growth rate v.s. m and h



Σ/ω shown here.



Link to type III

Recall co-orbital mass deficit

$$\delta m = 4\pi a \chi_s (\Sigma_e - \Sigma_g)$$

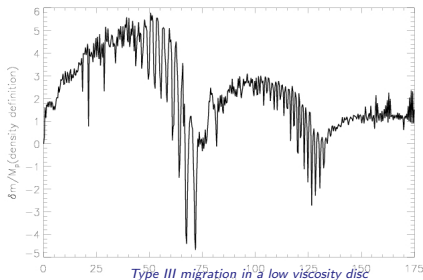
- ▶ Instability can increase δm by increasing Σ_e but not Σ_g (co-rotational modes are localised) \Rightarrow favouring type III. When vortex flows across co-orbital region, Σ_g increases and migration *may* stall.

Link to type III

Recall co-orbital mass deficit

$$\delta m = 4\pi a x_s (\Sigma_e - \Sigma_g)$$

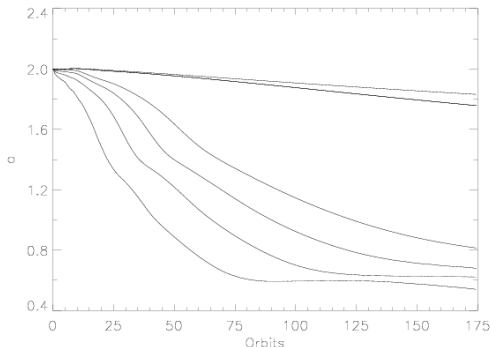
- ▶ Instability can increase δm by increasing Σ_e but not Σ_g (co-rotational modes are localised) \Rightarrow favouring type III. When vortex flows across co-orbital region, Σ_g increases and migration *may* stall.
- ▶ Can expect interaction when δm of order planet mass.





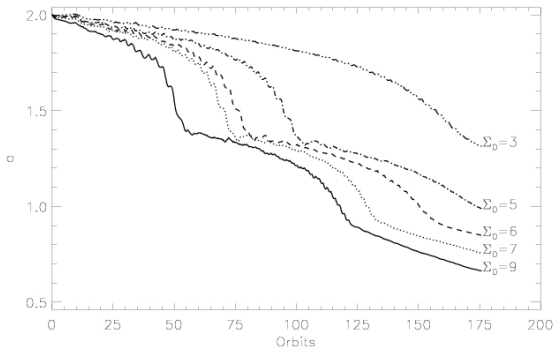
Implications of linear theory

Changing disc masses in standard viscous disc $\nu = 10^{-5}$



Top to bottom: $\Sigma \times 10^4 = 1, 2.5, 5, 7, 10, 15$

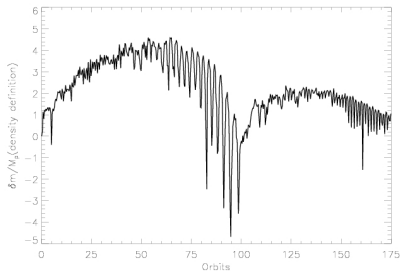
Growth rate independent of density scale. Higher density just means less time needed for vortex to grow sufficiently large for interaction.



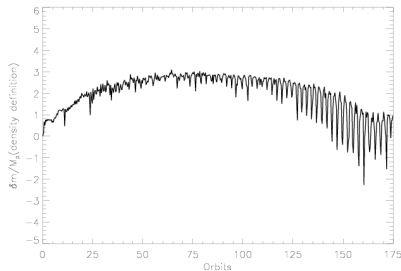


Implications of linear theory

In terms of co-orbital mass deficit...



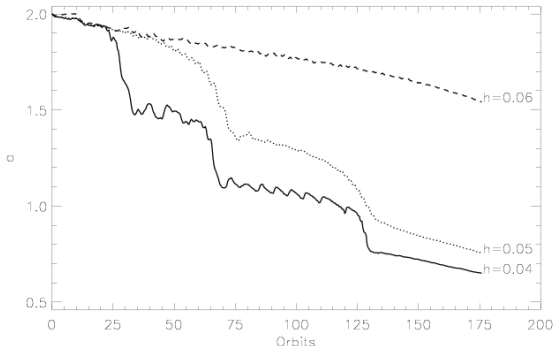
$$\Sigma_0 = 5$$



$$\Sigma_0 = 3$$

Implications of linear theory

$c_s^2 = T \propto h^2$. Lower temperature \Rightarrow stronger shocks \Rightarrow profile more unstable \Rightarrow shorter time-scale to vortex-planet interaction.



Require disc profile to be sufficiently extreme and have enough mass to trigger vortex-planet interaction, but the extent of migration during one episode is the same.

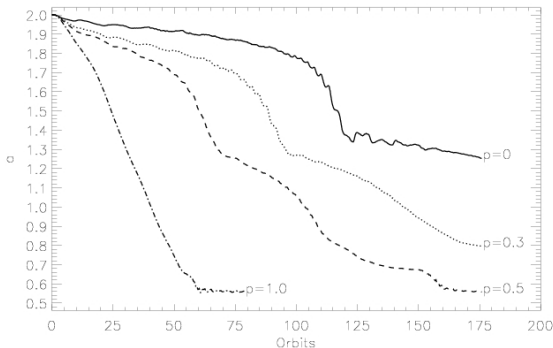


Vortex-triggered migration

- ▶ Migration may not stall after vortex-planet interaction if Σ_e increases relative to Σ_g . Possible if planet scattered to region of high density.
- ▶ Consider discs with $\Sigma \propto r^{-p}$. Note $\delta m(t=0) > 0$ in this case.

Vortex-triggered migration

- ▶ Migration may not stall after vortex-planet interaction if Σ_e increases relative to Σ_g . Possible if planet scattered to region of high density.
- ▶ Consider discs with $\Sigma \propto r^{-p}$. Note $\delta m(t=0) > 0$ in this case.

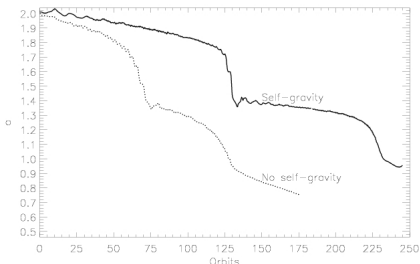


Vortices can trigger migration, needed for type III.

- ▶ Migration in low viscosity/inviscid discs is non-smooth due to shear instabilities associated with gap edge (vortensity minima).
- ▶ Provided an over-all picture of vortex-planet interaction: formation of unstable basic state via shocks, linear stability analysis and hydrodynamic simulations.
- ▶ Instability encourages type III by increasing co-orbital mass deficit. Vortex-planet interaction when $\delta m/M_p \sim 4\text{--}5$. Associated disruption of co-orbital vortensity structure.
- ▶ Vortex-induced migration stalls in uniform density discs but can act as trigger in $\Sigma \propto r^{-p}$ discs.

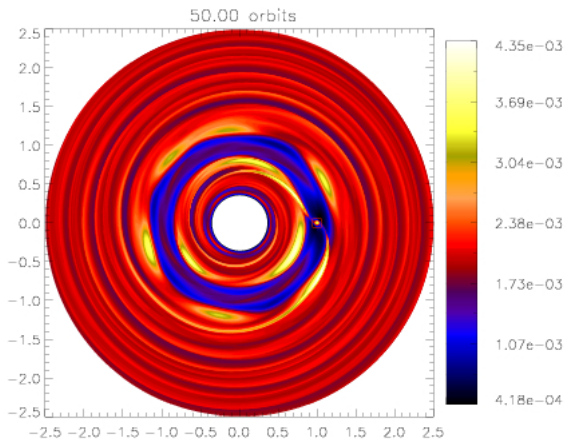
Future work: self-gravity

- ▶ Type III, or runaway migration recognised to operate in massive discs (few times MMSN), but conclusion reached using simulations without self-gravity.
- ▶ Fiducial case with $\Sigma = 7 \times 10^{-4}$ gives $Q(r_p) \simeq 5.6$. Need to have SG!



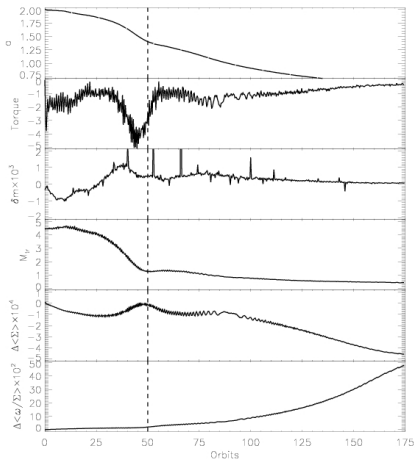
- ▶ Implement Li et al. (2009) Poisson solver to FARGO for high-resolution studies of co-orbital disc-planet interaction with self-gravity.

Thanks

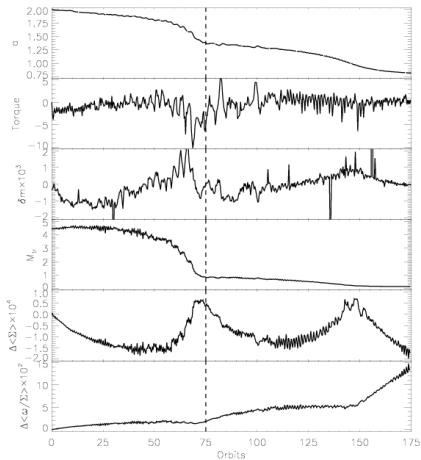


(FARGO with Li et al.'s Poisson solver.)

Bonus slide: evolution of co-orbital region



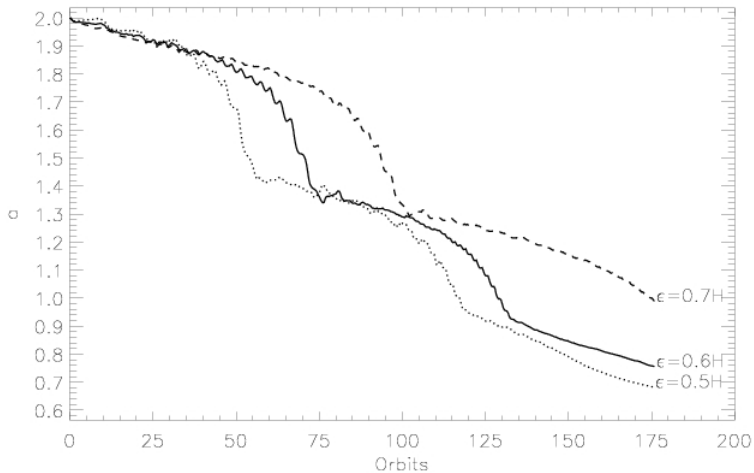
$$\nu_0 = 0.5$$



$$\nu_0 = 0$$

Bonus slide: effect of softening

$$\Phi_p = -\frac{M_p}{\sqrt{|\mathbf{x}-\mathbf{x}_p|^2+\epsilon^2}}$$

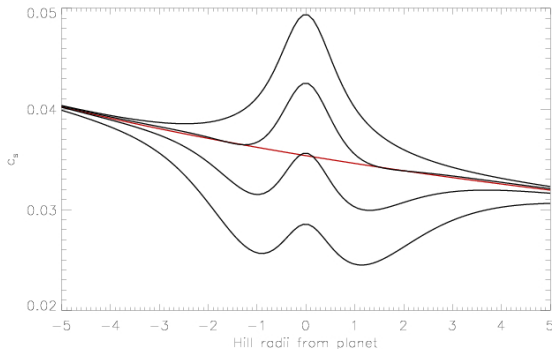


Bonus slide: special equation of state

Peplinski et al. (2008):

$$c_s = \frac{hr_s h_p r_p}{[(hr_s)^n + (h_p r_p)^n]^{1/n}} \sqrt{\Omega_s^2 + \Omega_p^2}$$

$n = 3.5$ and vary h_p to get temperature modifications close to planet.



Top to bottom (black curve) $h_p = 0.7, 0.6, 0.5, 0.4$. Red curve: local isothermal.

Bonus slide: special equation of state

